Cellular and Molecular Biology

Feng et al., Cell Mol Biol 2015, 61:2

Research Article Open Access

Absence of uPAR Protects against the Development of Atherosclerosis in LDL Receptor-Null Mice

Feng Su[1], Kathy R Kozak[1], Robin Farias-Eisner[1] and Srinivasa T Reddy[1,2,3]*

[1]Department of Obstetrics and Gynecology, University of California, Los Angeles, California, USA
[2]Department of Medicine, University of California, Los Angeles, California, USA
[3]Department of Molecular and Medical Pharmacology, University of California, Los Angeles, California, USA

Abstract

We have previously identified unrokinase plasminogen activator receptor [uPAR] as one of several genes differentially induced in human aortic endothelial cells [HAEC] by Oxidized-L-alpha-1-Palmitoyl-2-Arachidonoyl-sn-glycero-3-Phosphorylcholine [Ox-PAPC], which is a key biologically active component of oxidizedx low-density lipoprotein [Ox-LDL]. The role of uPAR in the development of atherosclerosis is not known. In this report, we show that uPAR message and protein are induced in HAEC within hours of Ox-PAPC treatment. We developed uPAR$^{-/-}$ mice on an LDLR$^{-/-}$ background [uPAR$^{-/-}$/LDLR$^{-/-}$] and show that uPAR plays a proatherogenic role in the aortic vascular milieu. When compared to LDLR$^{-/-}$ mice, uPAR$^{-/-}$/LDLR$^{-/-}$ mice fed a Western diet for 12 weeks had i] an anti-atherogenic serum lipid profile, ii] less atherogenic lipoproteins, iii] reduced accumulation of macrophages in the aortic sinus lesions, and iv] significantly reduced atherosclerosis in the entire aortic tree and the aortic sinus. Our results suggest, for the first time, that uPAR inhibition is a potential therapeutic approach to prevent atherosclerosis development.

Keywords: Urokinase plasminogen activator receptor; Atherosclerosis; Inflammation; Lipoproteins

Abbreviations: CVD: Cardiovascular Disease; uPAR: Unrokinase Plasminogen Activator Receptor; uPA: Unrokinase Plasminogen Activator; LDLR: Low Density Lipoprotein Receptor; HAEC: Human Aortic Endothelial Cells; Ox-PAPC: Oxidized-L-Alpha-1-Palmitoyl-2-Arachidonoyl-Sn-Glycero-3-Phosphorylcholine.

Introduction

Cardiovascular disease [CVD] is the leading cause of death in both men and women in the United States. Nearly three-fourths of all deaths from cardiovascular disease are due to heart attack or stroke caused by atherosclerosis, a chronic inflammatory disease of the arterial wall, characterized by the formation of lipid-laden lesions [1]. It is now established that the oxidation of low density lipoproteins [Ox-LDL] in the circulation resulting in the inflammatory responses by the artery wall endothelial cells and accumulation of macrophages in the artery wall are initial and critical steps in the development of atherosclerosis [2,3]. Identifying key genes involved in such early steps of atherosclerosis development and understanding their mechanism[s] of action are critical for discovering novel therapeutic targets in the fight against CVD.

We have previously identified unrokinase plasminogen activator receptor [uPAR] differentially induced in human aortic endothelial cells [HAEC] by Oxidized-L-alpha-1-Palmitoyl-2-Arachidonoyl-sn-glycero-3-Phosphorylcholine [Ox-PAPC], which is a key biologically active component of oxidized low-density lipoprotein [Ox-LDL] [4]. uPAR is a cell membrane-associated receptor of the serine protease family; uPA/uPAR system is implicated in plasmin generation and pericellular proteolysis. The exact role of uPA/uPAR system in the development of atherosclerosis is not known [5], but it has been demonstrated that uPA/uPAR system is expressed and active in all cells of the artery wall [6,7,8,9]. uPAR is highly expressed in human atherosclerotic lesions and it's expression correlates with severity of atherosclerosis. uPAR has also been shown to facilitate leukocyte-endothelial interactions. In this paper, we report the development and characterization [with respect to atherosclerosis] of uPAR$^{-/-}$/LDLR$^{-/-}$ mice.

Materials and Methods

Cell Culture

HAEC were isolated and cultured as described previously [10]. HAEC were plated at a density of 2×10^5 cells/cm^2 and were allowed to grow, forming a confluent monolayer in 2 days. The day before experiments, HAEC were shifted to M199 medium containing 10% lipoprotein deficient serum [LPDS]. Ox-PAPC at a concentration of 50 µg/ml was added to the cultures.

Real-Time PCR

Total RNA from cell cultures was extracted after 4 hours treatment with Ox-PAPC using the RNeasy kit [Qiagen, Valencia, CA, USA] according to manufacturer's protocol. Reverse transcription [RT] was performed with an Omniscript® Reverse Transcription Kit [Qiagen, Valencia, CA, USA] and cDNA was analyzed by qPCR using the SYBR Green Supermix [Bio-Rad, Hercules, CA, USA] in CFX96 Real-Time System [Bio-Rad, Hercules, CA, USA] following the manufacturer's instructions. Triplicate qPCR reactions were carried out in each sample. The following primers were used to detect human uPAR gene. Forward: CTGGAGCTTGAAAATCTGCC and Reverse: CGGCAGTCAATGAGGAAAGT.

Western Blot Analysis

HAECs were treated with Ox-PAPC at 50 ug/ml for 10 hours. Total

***Corresponding author:** Srinivasa T Reddy, Departments of Medicine, Molecular and Medical Pharmacology, Obstetrics and Gynecology, University of California, Los Angeles, CA 90095, USA. 10833 Le Conte Avenue, Los Angeles, CA 90095, USA, Tel: 1-310-206-3915; Fax: 310-206-3605; E-mail: sreddy@mednet.ucla.edu

Received December 14, 2015; **Accepted** December 28, 2015; **Published** December 31, 2015

Citation: Su F, Kozak KR, Farias-Eisner R, Reddy ST (2015) Absence of uPAR Protects against the Development of Atherosclerosis in LDL Receptor-Null Mice. Cell Mol Biol 61: 122.

cell proteins were collected after treatment in cell lysis buffer containing 0.1 mol/L NaCl, 5 mmol/L EDTA, 50 mmol/L sodium orthovanadate, 1% Triton X-100, and protease inhibitor tablet in 50 mmol/L Tris buffer [pH 7.5]. Twenty micrograms of total proteins were separated by SDS-PAGE and transferred onto nitrocellulose membrane and followed by incubation with primary antibody at 4°C in 5% skim milk and 0.1% Tween-20. Primary antibodies to human uPAR [R&D Systems, Minneapolis, MN, USA] and GAPDH were used at the manufacturer's recommended dilutions. Secondary antibody, anti-goat IgG was used at a dilution of 1:5,000.

Genotyping of uPAR$^{-/-}$/LDLR$^{-/-}$ mice

Total genomic DNA was isolated from 0.2 cm of mouse-tail using DNeasy Tissue kit [Qiagen, Valencia, CA, USA]. All PCR reactions were performed using the following conditions: 95°C for 15 seconds, 55°C for 1 min, 72°C for 1 min, total 30 cycles. The following primer sets and PCR product sizes were utilized for the genotyping analyses of LDLR$^{-/-}$/uPAR$^{-/-}$ mice. uPAR wild type allele: Forward primer GCTGGACACATTGGTACACA and Reverse primer CGCACACG-GTCTCTGTCAGG – 450 bp product. uPAR knockout allele: Forward primer GCTGGACACATTGGTACACA and the reverse primer TTCCGTCCTCCCTGCCGCCC – 180 bp product. LDLR wild type allele: Forward primer ACCCCAAGACGTGCTCCCAGGATGA and Reverse Primer CGCAGT GCTCCTCATCTGACTTGT-380 bp product. LDLR knockout allele: Forward primer AGGATCTCGTCGT-GACCCATGGCGA and Reverse primer GAGCGGCGATACCGTA-AAGCACGAGG – 200 bp product.

Animals and treatment

uPAR$^{-/-}$/LDLR$^{-/-}$ double knockout mice were generated at UCLA by crossing uPAR$^{-/-}$ mice with LDLR$^{-/-}$ mice [The Jackson laboratory, Bar Harbor, Maine, USA]. The background strain for both knockout mice strains was C57BL6/J. LDLR$^{-/-}$ and uPAR$^{-/-}$/LDLR$^{-/-}$ mice [n=15 per group, eight weeks of age] were fed a Western diet consisting of 21.2% fat, 0.2% cholesterol by weight [Harlan Teklad, WI, USA]. After 12 weeks on the Western diet, mice were sacrificed, and hearts, aortas and blood were collected. UCLA animal research committee approved all the experimental procedures.

Serum lipid analysis

Serum lipid levels [total cholesterol, unesterified cholesterol, triglycerides, HDL, non-HDL and free fatty acids] were performed in 96-well plates on a Biomek 2000 automated laboratory workstation [Beckman Coulter, Indianapolis, IN, USA] as described previously [11]. Measurements on serum samples were performed in triplicate with known control samples on each plate to ensure accuracy.

Aortic lesion analysis

The basal portion of the heart and the proximal aorta were harvested, washed in PBS to remove blood, embedded in Tissue-Tec OCT medium and stored at –80°C until sectioning. Serial 10-μm-thick cryosections from the middle portion of the ventricle to the aortic arch were collected and mounted on poly-D-lysine–coated slides. In the region from the appearance to the disappearance of the aortic valves, every other section was collected. Sections were stained with Oil Red O and hematoxylin and counterstained with fast green, and then examined by light microscopy for the identification of athermanous lesions. The mean area of lipid staining from 8-10 sections was determined for each mouse.

Quantification of atherosclerosis in descending aorta [en face analysis]

The aorta from arch to bifurcation was dissected from surrounding tissues and fixed in 4% formaldehyde. Then it was opened longitudinally, pinned onto black wax plates and stained with Sudan IV [Sigma-Aldrich, St. Louis, MO, USA]. The aortic lesion area and total aortic area were measured manually in a blinded fashion using Image-Pro Plus software.

Immunohistochemical analyses of atherosclerotic lesions

Immunohistochemical analyses of atherosclerotic lesions in the aortic root were performed as described previously [12]. Briefly, 10-μm-thick cryosections were fixed in acetone and incubated with a primary antibody, followed by incubation with biotinylated secondary antibody. Signals were detected with alkaline phosphatase substrate plus levamisole to inhibit endogenous alkaline phosphatase activity [Vector Laboratories, Burlingame, CA, USA]. Goat anti-mouse uPAR antibody [R&D Systems, Minneapolis, MN, USA] was used at 10 ug/ml working dilution, rat anti-mouse CD68 primary antibody [AbD Serotec, Raleigh, NC, USA] was used at 1:100 dilution, with an overnight incubation at 4°C. Rabbit anti-goat or Goat anti-rat biotinylated secondary antibodies [Jackson ImmunoResearch, West Grove, PA, USA] were used at 1:200 with 1 hour incubation at room temperature. In each section, the total area occupied by CD68-immunopositive macrophages was measured.

Plasma inflammatory index

HDL ability to interfere with LDL-induced monocyte migration was measured using the monocyte chemotactic activity [MCA] assay. LDL and HDL fractions were isolated from serum by fast-protein liquid chromatography. LDL-induced monocyte chemotactic activity and HDL anti-inflammatory properties were assessed as described previously [13]. Briefly, 100 μg of LDL, or 50 μg of HDL + 100 μg of control human LDL were added to a confluent monolayer of human aortic endothelial cells. Supernatants were collected and tested for monocyte chemotactic activity using a Neuroprobe chamber [Neuro Probe, Gaithersburg, MD, USA] with a polycarbonate filter of 5 μm pore size separating the upper and lower wells. Supernatants were added to the bottom chamber and freshly isolated monocytes to the top chamber. Membranes were fixed with 1% glutaraldehyde and stained with 0.1% Crystal Violet and the number of migrated monocytes was determined microscopically and expressed as mean ± SD.

Statistical analysis

Statistical significance was determined by student t test. A value of $p<0.05$ was considered statistically significant.

Results

Ox-PAPC induces uPAR expression in HAEC and uPAR is associated with atherosclerotic lesions in mice

We previously performed a suppression subtractive hybridization procedure to compare mRNA isolated from PAPC-treated HAEC with mRNA isolated from Ox-PAPC-treated cells [4] to identify genes that participate in the development of atherosclerosis. We identified uPAR as one of the Ox-PAPC-inducible genes in HAEC. We now show that uPAR message is induced in HAEC at 4 hours following Ox-PAPC treatment (Figure 1A). Moreover, uPAR protein is also induced by Ox-PAPC in HAEC when compared control HAEC (Figure 1B). We next examined whether uPAR is expressed in atherosclerotic lesion. We demonstrate that uPAR protein is highly expressed in the aortic root lesions of apoE$^{-/-}$ mice (Figure 1C).

Serum lipoproteins are significantly altered in uPAR$^{-/-}$/LDLR$^{-/-}$ mice

To determine the role of uPAR in the development of atherosclerosis,

we first intended to develop uPAR$^{-/-}$ mice on an apoE null background. However, due to the close proximity of uPAR and apoE loci the development of uPAR$^{-/-}$/apoE$^{-/-}$ mice was unsuccessful. We therefore chose to breed the uPAR$^{-/-}$ mice onto an LDLR null background. Viable uPAR$^{-/-}$/LDLR$^{-/-}$ mice were generated (Figure 2A). When uPAR$^{-/-}$/LDLR$^{-/-}$ mice were fed a Western diet the levels of TC, LDL, HDL, UC, and FFA were significantly [p< 0.01] altered when compared to the corresponding levels in LDLR$^{-/-}$ mice on a western diet (Figure 2B). Moreover, the lipoprotein cholesterol levels of HDL and LDL in uPAR$^{-/-}$/LDLR$^{-/-}$ mice were significantly less atherogenic when compared to LDLR$^{-/-}$ mice suggesting that uPAR deficiency is anti-atherogenic in LDLR$^{-/-}$ mice in a Western diet (Figure 2C).

uPAR deficiency protects against the development of diet-induced atherosclerosis in LDLR$^{-/-}$ mice

We next determined whether uPAR deficiency affected the development of atherosclerosis in LDLR$^{-/-}$ mice. Histological analysis of aortic root lesions showed that uPAR$^{-/-}$/LDLR$^{-/-}$ mice had significantly smaller aortic root lesions compared to LDLR$^{-/-}$ mice after 12 weeks on Western diet [260 vs. 388, p<0.0001, Figure 3A, and 3B]. To further determine the extent of atherosclerosis we performed en face analysis of the aortic tree and observed that uPAR$^{-/-}$/LDLR$^{-/-}$ mice had significantly reduced percent of lesion area when compared to LDLR$^{-/-}$ mice [2.0 vs. 7.9 %, p<0.001, Figure 3C and 3D].

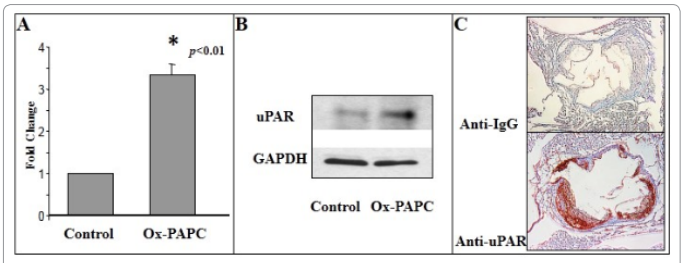

Figure 1: uPAR is an Ox-PAPC inducible gene and is highly expressed in atherosclerotic lesions. A. uPAR mRNA is induced by OX-PAPC in HAEC. Human aortic endothelial cells were exposed to OX-PAPC and harvested after 4 hours. Total RNA was isolated and subjected to Real-Time PCR analysis. B. uPAR protein is induced by Ox-PAPC in HAEC. Total protein lysates isolated from Ox-PAPC-treated HAEC were subjected to Western Blot analysis for uPAR. C. uPAR protein is highly expressed in the aortic root lesions of apoE$^{-/-}$ mice. Immunohistochemistry was performed for uPAR protein on cryostat sections obtained from the aortic root of 24 week-old apoE$^{-/-}$ mice.

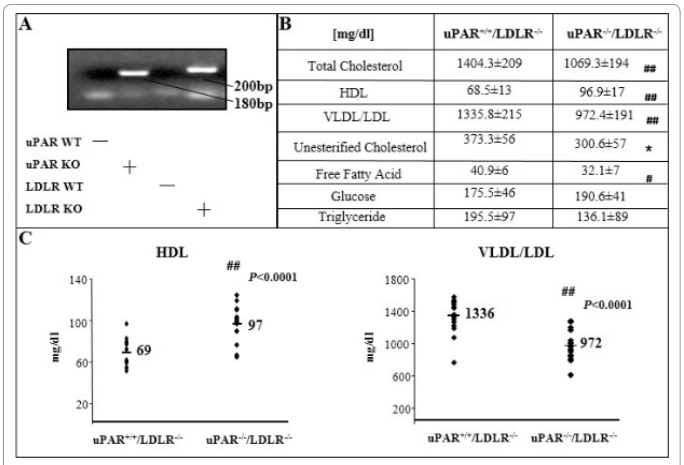

B [mg/dl]	uPAR$^{+/+}$/LDLR$^{-/-}$	uPAR$^{-/-}$/LDLR$^{-/-}$	
Total Cholesterol	1404.3±209	1069.3±194	##
HDL	68.5±13	96.9±17	##
VLDL/LDL	1335.8±215	972.4±191	##
Unesterified Cholesterol	373.3±56	300.6±57	*
Free Fatty Acid	40.9±6	32.1±7	#
Glucose	175.5±46	190.6±41	
Triglyceride	195.5±97	136.1±89	

Figure 2: Generation and characterization of uPAR$^{-/-}$/LDLR$^{-/-}$ mice. A. Generation of uPAR$^{-/-}$/LDLR$^{-/-}$ mice. Viable uPAR$^{-/-}$/LDLR$^{-/-}$ mice were generated. Figure shows genotyping of uPAR$^{-/-}$/LDLR$^{-/-}$ using the PCR protocol described under Materials and Methods. B. uPAR deficiency significantly alters serum levels of TC, LDL, HDL, UC, and FFA in LDLR$^{-/-}$ mice on a western diet. uPAR$^{+/+}$/LDLR$^{-/-}$ and uPAR$^{-/-}$/LDLR$^{-/-}$ mice (n=15 per group, eight weeks of age) were fed with Western Diet for 12 weeks. After 12 weeks treatment, the mice were bled and serum levels of total cholesterol, triglycerides, and HDL-cholesterol were determined as described in Materials and Methods. C. Lipoprotein cholesterol levels are positively affected in uPAR$^{-/-}$/LDLR$^{-/-}$ mice on a Western diet. Serum levels of HDL cholesterol and VLDL/LDL cholesterol were quantified as described under Materials and Methods. * P<0.01; # P<0.001; ## p<0.0001.

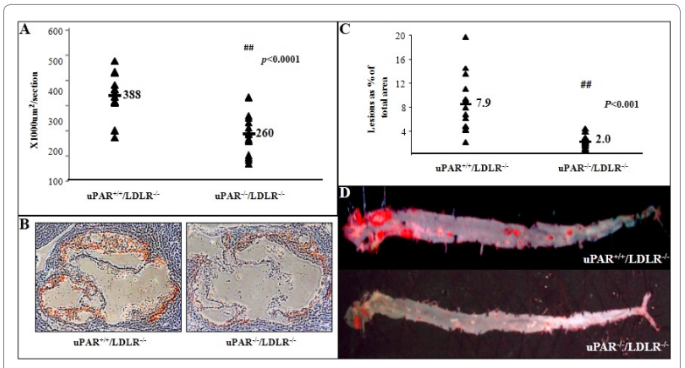

Figure 3: UPAR deficiency protects against the development of diet-induced atherosclerosis in LDLR$^{-/-}$ mice. A. Atherosclerotic lesion development at the aortic root in Western diet fed mice. Two groups of uPAR$^{+/+}$/LDLR$^{-/-}$ and uPAR$^{-/-}$/LDLR$^{-/-}$ mice (n=15 per group, eight weeks of age) were fed with Western Diet for 12 weeks. Each symbol represents the mean atherosclerotic lesion area calculated from 8-10 oil red O-stained sections spanning the aortic sinus of an individual mouse. Horizontal lines indicate mean percent lesion area for each group of animals. Significant differences were obeserved between the two groups (## p< 0.001). B. Representative oil red O-stained aortic sinus sections from uPAR$^{+/+}$/LDLR$^{-/-}$ and uPAR$^{-/-}$/LDLR$^{-/-}$ mice fed on Western diet for 12 weeks. C. Atherosclerosis in the descending aorta is suppressed in uPAR$^{-/-}$/LDLR$^{-/-}$ Western diet-fed mice. Each symbol represents the percent of total area of the indicated section of aorta that stained positively for Sudan IV in individual mouse maintained on Western diet for 12 weeks. Horizontal lines indicate mean percent lesion area in the indicated aortic section, including the aortic arch, thoracic aorta, abdominal aorta and total aorta (aortic arch + thoracic aorta + abdominal aorta), for each group of animals. Asterisks denote statistically significant differences between groups (## p < 0.001). Percentage of atherosclerosis lesions calculated from uPAR$^{-/-}$/LDLR$^{-/-}$ mice is "significant decrease from uPAR$^{+/+}$/LDLR$^{-/-}$ mice (2.0 vs.7.9, p < 0.001). D. Representative Sudan IV-stained aortas from the two groups.

uPAR deficiency results in anti-inflammtory lipoproteins in the circulation

Since uPAR$^{-/-}$/LDLR$^{-/-}$ mice carry less LDL-C and more HDL-C in the circulation (Figure 2C), we next examined whether the functional properties of HDL and LDL in the two groups of mice. We have previously described protocols to determine the inflammatory properties of HDL and LDL using an artery wall cell coculture method [10]. As seen in Figure 4A, HDL from uPAR$^{-/-}$/LDLR$^{-/-}$ mice was significantly [p<0.001] less pro-inflammatory when compared to HDL from LDLR$^{-/-}$ mice as indicated by uPAR$^{-/-}$/LDLR$^{-/-}$ HDL's ability to mitigate LDL-induced monocyte chemotactic activity. Furthermore, LDL from uPAR$^{-/-}$/LDLR$^{-/-}$ mice was significantly [p<0.001] less pro-inflammatory when directly assayed for chemotactic activity in cocultures of human artery wall cells in the absence of HDL (Figure 4B).

Atherosclerotic lesions from uPAR$^{-/-}$/LDLR$^{-/-}$ mice contain significantly less number of macrophages

To determine whether the anti-inflammatory nature of lipoproteins in the uPAR$^{-/-}$/LDLR$^{-/-}$ mice result in reduced monocyte chemotactic activity, sections of mouse aorta from the experiments described under Figure 3A were analyzed by immunohistochemistry for the presence of macrophages using CD-68 antibody

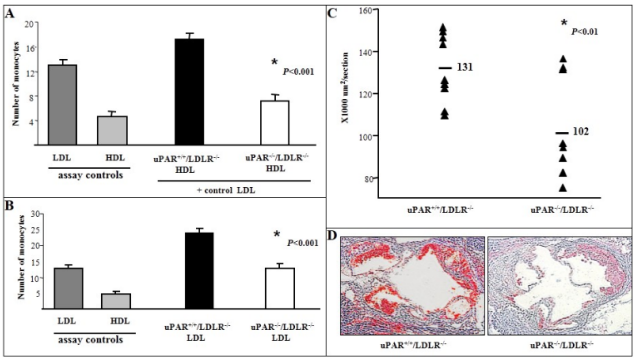

Figure 4: uPAR deficiency results in anti-inflammtory lipoproteins in the circulation and reduced acumulation of macrophages in the artery wall. A. LDL was added to cocultures of human artery wall cells in the absence or presence of HDL from uPAR$^{+/+}$/LDLR$^{-/-}$ and uPAR$^{-/-}$/LDLR$^{-/-}$ mice as described in the Methods. B. LDL from the two groups mice was added to cocultures of human artery wall cells in the absence of HDL and assayed for chemotactic activity as described in the Methods. Values are expressed as the mean±SEM of the number of migrated monocytes. C. uPAR$^{-/-}$/LDLR$^{-/-}$ mice accumulate significantly lower number of macrophage in atherosclerotic lesions compared to uPAR+/+/LDLR$^{-/-}$ mice. Sections of mouse aorta from the experiments described under Figure 3 were analyzed by immunohistochemistry for the presence of macrophages using CD-68 antibody and quantified as described in Materials and methods. D. Representative image of macrophage content in atherosclerotic plaques.

The aortic root lesions accumulated significantly less numbers of macrophages in uPAR$^{-/-}$/LDLR$^{-/-}$ mice compared to LDLR$^{-/-}$ mice [102 vs. 131, p<0.01, Figure 4C and 4D).

Discussion

Atherosclerosis is the underlying cause of vascular inflammatory diseases. The accumulation of oxidized lipids in the artery wall milieu initiates the recruitment of monocytes to the artery wall where they play a critical role in eliminating the toxic effects of oxidized lipids. However, based on a complex set of genetic and environmental mechanisms, the lipid loaded macrophages or foam cells can also initiate the earliest onset of atherosclerosis [1]. Understanding the molecular players that participate in such mechanisms will be important for developing therapeutic strategies for inhibiting the development of atherosclerosis.

We previously reported that oxidized phospholipids [e.g. Ox-PAC], the major pro-inflammatory constituents of Ox-LDL regulate the expression of a number of important genes in the artery wall cells including uPAR [4]. The uPA/uPAR system is comprised of the serine protease uPA and the cell membrane-associated receptor of uPA [uPAR] [14]. uPA binds with high affinity to its receptor uPAR and converts plasminogen to an active enzyme, plasmin, which in turn activates matrix metalloproteases responsible for extracellular matrix remodeling. uPA and uPAR are expressed by vascular endothelial cells, SMC, monocytes and macrophages [5].

The uPA/uPAR system plays an important role in the pathogenesis of vascular diseases [15]. In humans, uPAR and uPAR-bound uPA levels correlate with severity of atherosclerosis [16,17,18]. Among the two, uPA has been studied extensively with respect to atherosclerosis and vascular diseases [6,8,19,20]. Recent studies suggest that uPA over-expression contributes to the development, progression, and complications of atherosclerosis [6,8,20]. Plasma levels of uPA were found elevated in patients with unstable angina and correlated positively and associated with signs of plaque instability [21,22]. Interestingly, in uPA$^{-/-}$/apoE$^{-/-}$ mice, lack of uPA promotes progression and instability of mouse atherosclerotic lesions [23].

uPAR expression is elevated on monocytes from patients with acute myocardial infarction [24]. The role of uPAR on macrophage infiltration was examined using Raw264.7 cell lines expressing high levels of human uPA and uPAR [25]. Raw264.7 cells expressing human uPAR or both human uPAR and uPA, but not uPA alone, were detected in the aortic wall of apoE$^{-/-}$ mice, and no cells were detected in that of age-matched C57BL/6J mice after intravenous infusion of the cells [25]. More recently, it has been reported that uPAR regulates monocyte migration and is associated with accelerated atherosclerosis in apoE$^{-/-}$ mice [26]. uPA has also been shown to regulate cell migration and invasion by coupling to uPAR [27]. The direct role of uPAR in the development of atherosclerosis has not been studied. We show that uPAR is an Ox-PAPC inducible gene in HAEC (Figure 1) and is also highly expressed in atherosclerotic lesions of apoE null mice (Figure 1). Our results showing that there is a reduced accumulation of monocyte/macrophages in the artery walls of uPAR$^{-/-}$/LDLR$^{-/-}$ mice (Figure 4) are in agreement with the previous reports suggesting a role for uPAR in monocyte chemotaxis/migration [25,26].

Absence of uPAR in Western diet fed LDLR$^{-/-}$ mice resulted in an average 33% reduction of atherosclerosis in the aortic sinus (Figure 3A) and an average 75% reduction in atherosclerosis measured as a percent of total area in the entire aortic tree (Figure 3C). These results underscore the role of uPAR in the development of diet-induced atherosclerosis. Although we were initially planning to study the role of uPAR in a spontaneous [non-diet induced] hyperlipidemic mouse, we were unable to accomplish this due to feasibility issues. Since uPAR and apoE gene loci are close to one another [Ensembl cytogenetic band: 19q13.31 and 19q13.32, respectively], it was not possible to obtain double knockout by breeding methodology.

One intriguing finding from the current study is the effect uPAR had on lipid and lipoprotein metabolism. The absence of uPAR in uPAR$^{-/-}$/LDLR$^{-/-}$ mice resulted in a diet-induced lipid profile that was significantly less atherogenic when compared to LDLR$^{-/-}$ mice (Figure 2). We do not have a direct explanation for these observations cells. These results demonstrate that absence of uPAR prevented the accumulation [and/or generation] of pro-inflammatory lipoproteins in the circulation.

In conclusion, our results demonstrate, for the first time, that the absence of uPAR alters lipid and lipoprotein properties, prevents macrophage accumulation in the artery wall, and reduces diet-induced atherosclerosis in LDLR$^{-/-}$ mice. These results suggest that inhibition of uPAR expression and/or function has therapeutic potential for the treatment of CVD. But we speculate that this is most likely a homeostasis effect of reduced inflammation in the circulation. As noted in Figure 4, uPAR deficiency in LDLR$^{-/-}$ mice mitigated the diet-induced accumulation of pro-inflammatory lipoproteins (Figure 4A and 4B) measured in a bioassay that quantifies the monocyte chemotaxis caused by the effect of pro-inflammatory lipoproteins on artery wall

Acknowledgements

The authors thank Susan Hama, Sarada Charugundla and Victor Grijalva for their technical support. This work was supported by funds from the Women's Endowment, the Carl and Roberta Deutsch Family Foundation, the Joan English Fund for Women's Cancer Research, and the National Institutes of Health National Heart, Lung, and Blood Institute [Grant HL-082823].

References

1. Mestas, J. & Ley, k.
Monocyte-Endothelial Cell Interactions in the Development of Atherosclerosis. *Trends Cardiovasc Med.* 2008, **18**: 228-232.

2. Navab, M., Hama, S. Y., Cooke, C. J., Anantharamaiah, G. M., Chaddha, M., Jin, L., Subbanagounder, G., Faull, K. F., Reddy, S. T., Miller, N. E. & Fogelman, A. M.
Normal high density lipoprotein inhibits three steps in the formation of mildly oxidized low density lipoprotein: step 1.
J Lipid Res. 2000, **41**: 1481-1494

3. Navab, M., Hama, S. Y., Anantharamaiah, G. M., Hassan, K., Hough, G. P., Watson, A. D., Reddy, S. T., Sevanian, A., Fonarow, G. C. & Fogelman, A. M.
Normal high density lipoprotein inhibits three steps in the formation of mildly oxidized low density lipoprotein: steps 2 and 3.
J Lipid Res. 2000, **41**: 1495-1508.

4. Reddy, S. T., Grijalva, V., Ng, C., Hassan, K., Hama, S., Mottahedeh, R., Wadleigh, D. J., Navab, M. & Fogelman, A. M.
Identification of genes induced by oxidized phospholipids in human aortic endothelial cells. *Vascul Pharmacol*. 2002, **38**: 211-218.

5. Fuhrman, B.
The urokinase system in the pathogenesis of atherosclerosis.
Atherosclerosis 2012, **222**: 8-14.

6. Kienast, J., Padró, T., Steins, M., Li, C. X., Schmid, K. W., Hammel, D., Scheld, H. H. & van de Loo, J. C.
Relation of urokinase-type plasminogen activator expression to presence and severity of atherosclerotic lesions in human coronary arteries.
Thromb Haemost. 1998, **79**: 579–586

7. Lupu, F., Heim, D. A., Bachmann, F., Hurni, M., Kakkar, V. V. & Kruithof, E. K. Plasminogen activator expression in human atherosclerotic lesions.
Arterioscler Thromb Vasc Biol. 1995, **15**: 1444-1455.

8. Padró, T., Emeis, J. J., Steins, M., Schmid, K. W. and Kienast, J.
Quantification of plasminogen activators and their inhibitors in the aortic vessel wall in relation to the presence and severity of atherosclerotic disease.
Arterioscler Thromb Vasc Biol. 1995, **15**: 893-902.

9. Shen, G. X.
Vascular cell-derived fibrinolytic regulators and atherothrombotic vascular disorders.
Int J Mol Med. 1998, **1**: 399-408.

10. Navab, M., Liao, F., Hough, G. P., Ross, L. A., Van Lenten, B. J., Rajavashisth, T. B., Lusis, A. J., Laks, H., Drinkwater, D. C. & Fogelman, A, M.
Interaction of monocytes with cocultures of human aortic wall cells involves interleukins 1 and 6 with marked increases in connexin43 message.
J Clin Invest. 1991, **87**: 1763-1772.

11. Mehrabian, M., Qiao, J. H., Hyman, R., Ruddle, D., Laughton, C. & Lusis, A. J.
Influence of the ApoA-II Gene Locus on HDL Levels and Fatty Streak Development in Mice.
Arterioscler Thromb. 1993, **13**: 1-10.

12. Shih, D. M., Xia, Y. R., Wang, X. P., Miller, E., Castellani, L. W., Subbanagounder, G., Cheroutre, H., Faull, K. F., Berliner, J. A., Witztum, J. L. & Lusis, A. J.
Combined Serum Paraoxonase Knockout/Apolipoprotein E Knockout Mice Exhibit Increased Lipoprotein Oxidation and Atherosclerosis.
J Biol Chem. 2000, **275**: 17527-17535.

13. Ng, C. J., Wadleigh, D. J., Gangopadhyay, A., Hama, S., Grijalva, V. R., Navab, M., Fogelman, A. M. & Reddy, S. T.
Paraoxonase-2 is a ubiquitously expressed protein with antioxidant properties and is capable of preventing cell-mediated oxidative modification of low density lipoprotein.
J Biol Chem. 2001, **276**: 44444-44449.

14. Mazar, A. P., Henkin, J. & Goldfarb, R. H.
The urokinase plasminogen activator system in cancer: implications for tumor angiogenesis and metastasis.
Angiogenesis 1999, **3**: 15-32.

15. Nicholl, S. M., Roztocil, E. & Davies, M. G.
Plasminogen activator system and vascular disease.
Curr Vasc Pharmacol. 2006, **4**: 101-116.

16. Pawlak, K., Pawlak, D. & My´sliwiec, M.
Urokinase-type plasminogen activator and metalloproteinase-2 are independently related to the carotid atherosclerosis in haemodialysis patients.
Thromb Res. 2008, **121**: 543-548.

17. Pawlak, K., Mysliwiec, M. & Pawlak, D.
The urokinase-type plasminogen activator/ its soluble receptor system is independently related to carotid atherosclerosis and associated with CC-chemokines in uraemic patients.
Thromb Res. 2008, **122**: 328-335.

18. Steins, M. B., Padró, T., Schwaenen, C., Ruiz, S., Mesters, R. M., Berdel, W. E. & Kienast, J.
Overexpression of urokinase receptor and cell surface urokinase-type plasminogen activator in the human vessel wall with different types of atherosclerotic lesions.
Blood Coagul Fibrinolysis 2004, **15**: 383-391.

19. Falkenberg, M., Tom, C., DeYoung, M. B., Wen, S., Linnemann, R. & Dichek, D. A.
Increased expression of urokinase during atherosclerotic lesion development causes arterial constriction and lumen loss, and accelerates lesion growth.
Proc Natl Acad Sci USA. 2002, **99**: 10665-10670.

20. Noda-Heiny, H., Daugherty, A. & Sobel, B. E.
Augmented urokinase receptor expression in atheroma.
Arterioscler Thromb Vasc Biol. 1995, **15**: 37-43.

21. Edsfeldt, A., Nitulescu, M., Grufman, H., Grönberg, C., Persson, A., Nilsson, M., Persson, M., Björkbacka, H. & Gonçalves, I.
Soluble urokinase plasminogen activator receptor is associated with inflammation in the vulnerable human atherosclerotic plaque.
Stroke 2012, **43**: 3305-3312.

22. Gyöngyösi, M., Glogar, D., Weidinger, F., Domanovits, H., Laggner, A., Wojta, J., Zorn, G., Iordanova, N. & Huber, K.
Association between plasmin activation system and intravascular ultrasound signs of plaque instability in patients with unstable angina and non-st-segment elevation myocardial infarction.
Am Heart J. 2004, **147**: 158-164.

23. Dellas, C., Schremmer, C., Hasenfuss, G., Konstantinides, S. V. & Schäfer, K.
Lack of urokinase plasminogen activator promotes progression and instability of atherosclerotic lesions in apolipoprotein E-knockout mice.
Thromb Haemost. 2007, **98**: 220-227.

24. May, A. E., Schmidt, R., Kanse, S. M., Chavakis, T., Stephens, R. W., Schömig, A., Preissner, K. T. & Neumann, F. J.
Urokinase receptor surface expression regulates monocyte adhesion in acute myocardial infarction.
Blood 2002, **100**: 3611-3617.

25. Gu, J. M., Johns, A., Morser, J., Dole, W. P., Greaves, D. R. & Deng, G. G.
Urokinase plasminogen activator receptor promotes macrophage infiltration into the vascular wall of ApoE deficient mice.
J Cell Physiol. 2005, **204**: 73-82.

Chen, W., Jin, W. Q., Chen, L. F., Williams, T., Zhu, W. L. & Fang, Q.
Urokinase receptor surface expression regulates monocyte migration and is associated with accelerated atherosclerosis.
Int J Cardiol. 2012, **161**:103-110.

26. Pliyev, B. K., Antonova, O. A. & Menshikov, M.
Participation of the urokinase-type plasminogen activator receptor (uPAR) in neutrophil transendothelial migration.
Mol Immunol. 2011, **48**: 1168-1177.